Cellulose (2020) 27:6617–6628
https://doi.org/10.1007/s10570-020-03227-1

ORIGINAL RESEARCH

Preparation of cellulose nanocrystal-dressed fluorinated polyacrylate latex particles via RAFT-mediated Pickering emulsion polymerization and application on fabric finishing

Jianhua Zhou · Xueli Wang · Yannan Li · Hong Li · Kun Lu

Received: 7 January 2020 / Accepted: 9 May 2020 / Published online: 20 May 2020

Abstract Cellulose nanocrystal-dressed fluorinated polyacrylate latex particles were prepared via RAFT-mediated Pickering emulsion polymerization using cellulose nanocrystals (CNCs) modified with amphiphilic polymers as Pickering stabilizers. The main work was to study the effect of pH value and the amount of fluorinated monomer on emulsion polymerization and finished fabric properties. The monomer conversion increased first and then decreased as the pH and the amount of fluorine monomer increased, while a reverse trend was noted for the particle size and particle size distribution. The results obtained from TEM verified that the latex particles presented a spher-like mophology with a well-defined core–shell structure. ^{1}H-NMR and FT-IR spectroscopy were employed to study the chemical structure of cellulose nanocrystal-dressed fluorinated polyacrylate latex particles. The SEM and EDX analysis indicated that cellulose nanocrystal-dressed fluorinated polyacrylate latex particles were successfully adhered to the fiber surface and the finished fabric presented a relatively rough surface morphology. The contact angle results exhibited the finished fabric had excellent water and oil resistance.

J. Zhou (✉) · X. Wang · Y. Li · H. Li
College of Bioresources Chemical and Materials Engineering, Shaanxi University of Science and Technology, Xi'an 710021, China
e-mail: zhoujianh@21cn.com

J. Zhou · X. Wang · Y. Li · H. Li
National Demonstration Center for Experimental Light Chemistry Engineering Education (Shaanxi, University of Science and Technology), Xi'an 710021, China

K. Lu
School of Arts and Science, Shaanxi University of Science and Technology, Xi'an 710021, China

Graphic abstract

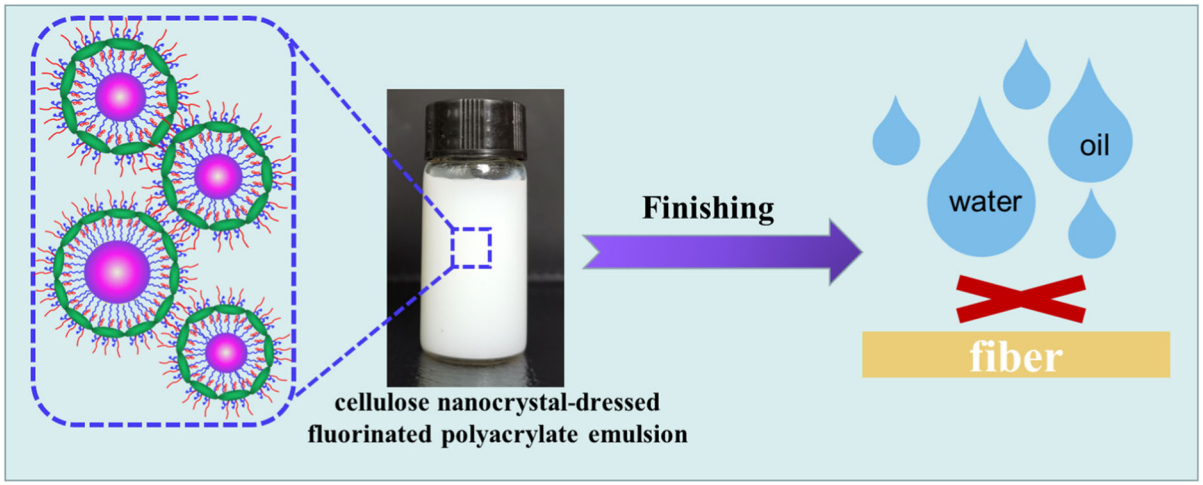

Keywords Cellulose nanocrystals · RAFT-mediated pickering emulsion polymerization · Fluorinated polyacrylate · Water and oil proof agent

Introduction

Polymeric materials have recently attracted considerable interest for an ever-increasing range of applications, including automobile, packaging, electronics, and biotechnology industries (Clélia and Bruno 2014; Wang et al. 2015; Zhou et al. 2018; Scaffaro et al. 2016; Moustafa et al. 2019). Among various types of polymers, fluorinated polyacrylate polymer is considered as one of the most promising candidates because it not only has many virtues of fluorinated polymer, but also retains the strong adhesion and good film-forming performance of polyacrylate (Lv et al. 2016).

Much research has shown long-chain fluorinated polyacrylate polymers have excellent water–oil resistance, chemical and thermal stability, which are associated with the unique properties and structure of the fluorine atom (Xu et al. 2014; Zhang et al. 2016, 2014; Yao et al. 2019). However, the main drawback of longer perfluoroalkyl chains (> C8) is that they have shown a potential health hazard due to the difficulty of degradation and possible bioaccumulation (Chen et al. 2015a; Kannan et al. 2002; Martin et al. 2004), which may limit their application potential in polyacrylate polymers. Concerning the environment effect, shorter perfluorinated alkyl chains, such as those studied in this work, have attracted a great attention. Unfortunately, the statistical copolymer with shorter perfluoroalkyl chains has lower surface energies than their longer analogues. It means that they are less effective in repelling water and oil (Chen et al. 2015a). In order to circumvent such disadvantages, a wide range of inorganic nanoparticles, including nano-SiO_2 (Zhou et al. 2015), nano-TiO_2 (Zhou et al. 2014b), and POSS (Liang et al. 2018), have been incorporated into the polymer matrices to improve the water–oil resistance of fluorinated polyacrylate. Despite the promising results achieved, these inorganic nanoparticles could not avoid the constraint of nonrenewable resources and hard biodegradation. To overcome the previously described limitation and realize the concept of sustainable development, the demand for the fabrication of "green" fluorinated polyacrylate composites through the biomass-based materials is imperative.

Needle-shaped cellulose nanocrystals (CNCs) with a characteristic diameter of 1–100 nm and a length of 100–200 nm, are renewable and biodegradable (Chen et al. 2018; Li et al. 2018; Cherhal et al. 2016). Over the last decades, CNCs have aroused great interest due to their specific chemical and physical properties such as lightweight, relatively low cost, high aspect ratio, and high Young's modulus (Habibi et al. 2010; Ng et al. 2015; El-Fattah et al. 2018), which renders them useful for a wide range of applications, including membrane support materials (Clélia and Bruno 2014),

energy devices (Du et al. 2017b), foams (Mougel et al. 2019) and packaging materials (Li et al. 2015). In recent years, researchers have focused on the incorporation of CNCs into polymer matrices by the Pickering emulsion polymerization method to achieve CNC-polymer nanocomposites with improved properties. However, the drawback of CNCs is that they have poor compatibility with hydrophobic polymers due to the primarily hydrophilic nature (Lizundia et al. 2016). Thus, the modified CNCs are mainly employed as stabilizers in Pickering emulsion polymerization. For example, Werner et al. (2017) prepared polystyrene/CNC core–shell composite microparticles stabilized by acetylated cellulose nanocrystals via Pickering emulsion polymerization. Tang et al. (2019) used cinnamoyl chloride modified CNCs as Pickering stabilizers to produce polydopamine microcapsules for essential oil and pesticides encapsulation. Errezma et al. (2018) used aldehyde-functionalized CNCs as Pickering stabilizers for surfactant-free emulsion polymerization of an acrylic monomer. Moreover, Du et al. (2017a) successfully synthesized PS/CNC composite microspheres, using 18-C alkyl chains modified CNCs as Pickering emulsion stabilizers.

It can be noticed that in all the above instances, the modified CNCs as Pickering emulsifiers have no reactive surface groups, and are attached to the polymers only by physical absorption or electrostatic interaction, which may impede the development of CNC-based composites with high potential for comprehensive applications. Rather than using noncovalent interaction, the association of nanoparticles with polymers through the covalent interaction is a suitable strategy for preparing polymer nanocomposite materials. The novelty of our previous work is that CNCs can be incorporated into polymer through covalent interactions. For example, we chose a "marcro-RAFT agent assisted" strategy to graft polyacrylic acid (AA) onto cellulose nanocrystal (CNC-g-PAA), then it served as a stabilizer and a chain transfer agent to prepare the CNC modified fluorinated polyacrylate. The results showed that the mechanical property and water–oil resistance of the nanocomposite latex films were dramatically improved (Yao et al. 2019). In the recent research, we had reported to use the CNCs grafted with amphipathic triblock copolymer poly(2-(dimethylamino) ethyl methacrylate)-b-poly(glycidyl methacrylate)-b-poly(hexafluorobutyl acrylate) (PDMAEMA-b-PGMA-b-PHFBA) as Pickering stabilizers for polymerization of fluoroacrylate via RAFT process. In this system, poly(2-(dimethylamino) ethyl methacrylate)-g-CNC-g-poly(hexafluorobutyl acrylate) (PDMAEMA-g-CNC-g-PHFBA) particles with hydrophilic PDMAEMA segments and hydrophobic PHFBA segments can self-assemble to form stable micelles in water. When the polymerization occurs, the PHFBA segments with RAFT active chain end located in the micelle interior can further mediate the polymerization of monomers inside, and finally were covalently anchored onto the latex particle surface (Zhou et al. 2013), while the hydrophilic PDMAEMA segments extended into the aqueous phase to form a hydrophilic shell around the particles (Zhou et al. 2019). Ultimately, the purpose of combining CNCs with polymers by more stable covalent bonds is realized. We had systematically explored the formation mechanism of cellulose nanocrystal-dressed fluorinated polyacrylate latex particles. Therefore, in this work, we followed this strategy to investigate detailedly the effect of pH value and amount of hexafluorobutyl acrylate (HFBA) on emulsion polymerization. Subsequently, cellulose nanocrystal-dressed fluorinated polyacrylate emulsion was used as a fabric finishing agent, and the water and oil resistance properties of the finished fabrics were investigated.

Experimental

Materials

2, 2′-Azobis (2-methylpropionamidine) dihydrochloride (AIBA, initiator) was obtained from Shanghai Aladdin Reagent Co. Ltd. (China), analytically pure and used as received. Hexafluorobutyl acrylate (HFBA, monomer), supplied by Harbin Xuejia Fluorosilicide Co. Ltd. (China), analytically pure and was passed through an alkaline alumina chromatographic column to remove inhibitor before use. Butyl acrylate (BA, monomer) and methyl methacrylate (MMA, monomer), chemically pure, were received from Tianjin Kemiou Chemical Reagent Co. Ltd. (China). BA and MMA were washed with sodium hydroxide (NaOH) aqueous solution to remove the phenolic inhibitor and then distilled under reduced pressure.

Poly(2-(dimethylamino) ethyl methacrylate)-g-CNC-g-poly(hexafluorobutyl acrylate) (PDMAEMA-g-CNC-g-PHFBA) was prepared according to a published procedure (Zhou et al. 2019).

Synthesis of cellulose nanocrystal-dressed fluorinated polyacrylate latex particles

The synthesis recipes were listed in Table 1. The typical preparation procedure and reaction conditions were as follows: the modified CNC suspension solution was prepared by dispersing PDMAEMA-g-CNC-g-PHFBA particles (0.07 g) in distilled water via sonication. Thereafter, HFBA (0.70 g, 2.96 mmol), BA (3.78 g, 29.5 mmol) and MMA (2.52 g, 2.52 mmol) were added to the modified CNC suspension solution and ultrasonicated for 6 min to form Pickering emulsion. Then, the emulsion was transferred to a three-necked glass reactor with a mechanical stirrer, and purged with argon gas under continuous stirring for 30 min. The polymerization was conducted at 75 °C by adding initiator aqueous solution (0.07 g (0.258 mmol) of AIBA dissolved in 2.00 mL deionized water) within 30 min. The reaction mixture was kept at 75 °C for 2 h.

In the sample code, "S" indicates different pH values, "P" indicates different contents of HFBA.

Fabric treatment

The cotton fabrics were padded through two dips and nips (70–80% wet pick up) in cellulose nanocrystal-dressed fluorinated polyacrylate emulsion of 70 g/L. The finished fabrics were dried at 80 °C for 3 min and then cured at 170 °C for 3 min.

Characterization

The pH value measurements were performed on a pH-meter (PHS-25) with an E-201-C pH composite electrode. ^{1}H-NMR spectrum was recorded on a Bruker 400 MHz spectrometer (ADVANCE III) after dissolution of sample in $CDCl_3$. FT-IR spectrum was obtained by a Bruker FT-IR spectrometer (VERTEX 70) in a scanning range from 400 to 4000 cm^{-1}. Monomer conversion and gel rate were determined by gravimetric analysis after drying the samples at 120 °C overnight. The Malvern Nano ZS instrument (Nano ZS 90) was employed to perform the measurement of the zeta potential, particle size and particle size distribution of the latex particles synthesized at different pH values. The contact angle test was performed with the sessile drop method using a goniometer (OCA-20) drop-shape tensiometer fitted with a microsyringe at room temperature. Transmission electron microscopy (TEM) images of latex particles were taken in transmission electron microscope (Tecnai G2-F20 S-TWIN) operated at 200 kV. Scanning electron microscopy (SEM, Hitachi S-4800) and energy dispersive X-ray (EDX) spectroscope were used to observe the surface morphology of the fabric and analyze its composition with an acceleration voltage of 20 kV.

Table 1 Recipes for cellulose nanocrystal-dressed fluorinated polyacrylate latex particles

Sample	S1	S2	S3	S4	S5	P1	P2	P3	P4	P5	P6	P7
PDMAEMA-*g*-CNC-*g*-PHFBA/g	0.07	0.07	0.07	0.07	0.07	0.07	0.07	0.07	0.07	0.07	0.07	0.07
pH value	1.07	2.06	2.97	4.86	6.85	2.06	2.06	2.06	2.06	2.06	2.06	2.06
AIBA/g	0.07	0.07	0.07	0.07	0.07	0.07	0.07	0.07	0.07	0.07	0.07	0.07
MMA/g	2.52	2.52	2.52	2.52	2.52	2.52	2.52	2.52	2.52	2.52	2.52	2.52
BA/g	3.78	3.78	3.78	3.78	3.78	3.78	3.78	3.78	3.78	3.78	3.78	3.78
HFBA/g	0.70	0.70	0.70	0.70	0.70	0.00	0.42	0.56	0.70	0.84	0.98	1.12
Distilled water/mL	33.00	33.00	33.00	33.00	33.00	33.00	33.00	33.00	33.00	33.00	33.00	33.00

Results and discussion

Synthesis and characterization of cellulose nanocrystal-dressed fluorinated polyacrylate latex particles

Cellulose nanocrystals (CNCs) were modified with the amphiphilic polymers to improve their dispersibility and wettability. Then, cellulose nanocrystal-dressed fluorinated polyacrylate latex particles were prepared by RAFT-mediated Pickering emulsion polymerization using poly(2-(dimethylamino) ethyl methacrylate)-g-CNC-g-poly(hexafluorobutyl acrylate) (PDMAEMA-g-CNC-g-PHFBA) particles as Pickering stabilizers and mixed monomers consisting of methyl methacrylate (MMA), n-butyl acrylate (BA) and hexafluorobutyl acrylate (HFBA) as oil phase, following the methodology described in Scheme 1.

The chemical structure of cellulose nanocrystal-dressed fluorinated polyacrylate latex particles was characterized by FT-IR spectroscopy as displayed in Fig. 1a. The bands at 2962 cm^{-1} and 2875 cm^{-1} can be attributed to stretching vibration peaks of $–CH_3$ and $–CH_2$. The vibration of C=O bonds appears at 1735 cm^{-1}, and the peaks at 1459 cm^{-1} and 1386 cm^{-1} belong to the in-plane deformation absorption peaks of methyl and methylene. Additionally, the characteristic absorption peak of C–F located at 1235 cm^{-1}. The band at 1165 cm^{-1} originates from the –C–O– stretching vibration of esters. The chemical structure of cellulose nanocrystal-dressed fluorinated polyacrylate latex particles was also demonstrated by ^{1}H-NMR spectrum (Fig. 1b). The signals at 5.25 ppm and 4.46 ppm originate from the (–CHF) protons and ($–CH_2CF_2$) protons of PHFBA segments, respectively. The feature signal of ($–O–CH_2CH_2CH_2CH_3$) in PBA chains is found at 4.05 ppm. Peak at 3.64 ppm belongs to ($–O–CH_3$) in the PMMA segments. Moreover, The characteristic peak of ($–N(CH_3)_2$) in PMDAEMA segments appears at 2.28 ppm. FT-IR and ^{1}H-NMR spectroscopy results indicated that all monomers had taken part in the emulsion polymerization and cellulose nanocrystal-dressed fluorinated polyacrylate latex particles were successfully prepared. Figure 1c is the TEM image of cellulose nanocrystal-dressed fluorinated polyacrylate latex particles with 10 wt% of HFBA at pH = 2.06. The latex particles are regular sphere with a well-defined core–shell structure of diameter about 150 nm. The gray region inside the latex particle is filled with fluorinated polyacrylate core, whereas the dark region at the periphery of the latex particle is modified CNC particle shell. This further proved that the modified CNC nanoparticles as

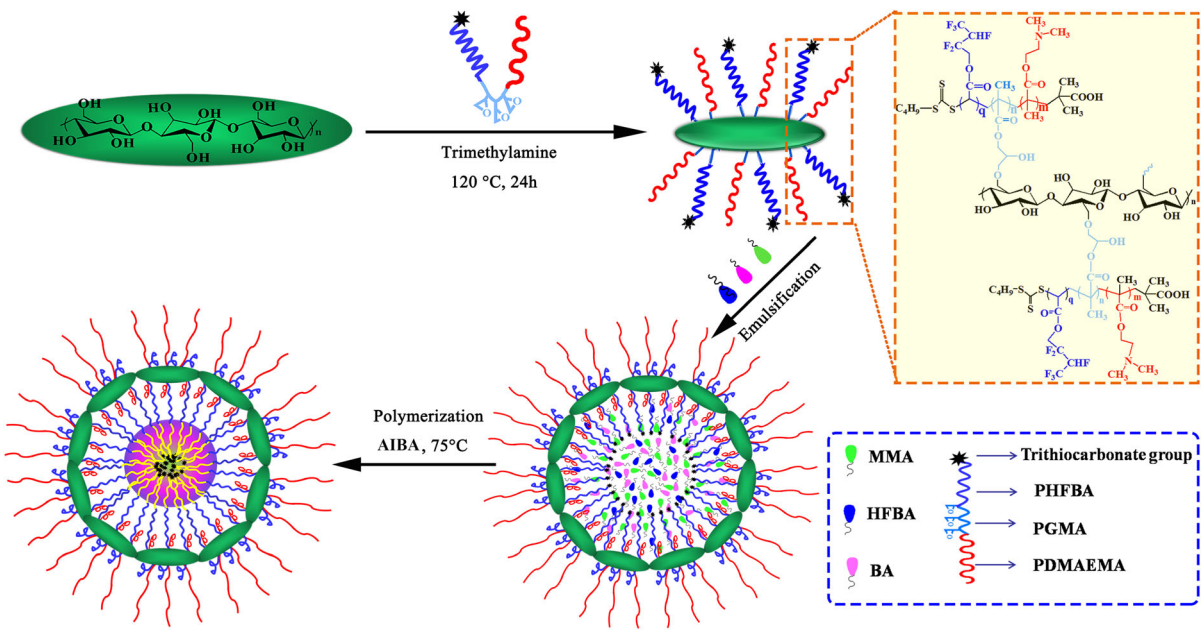

Scheme 1 Schematic representation of the synthesis of cellulose nanocrystal-dressed fluorinated polyacrylate latex particles

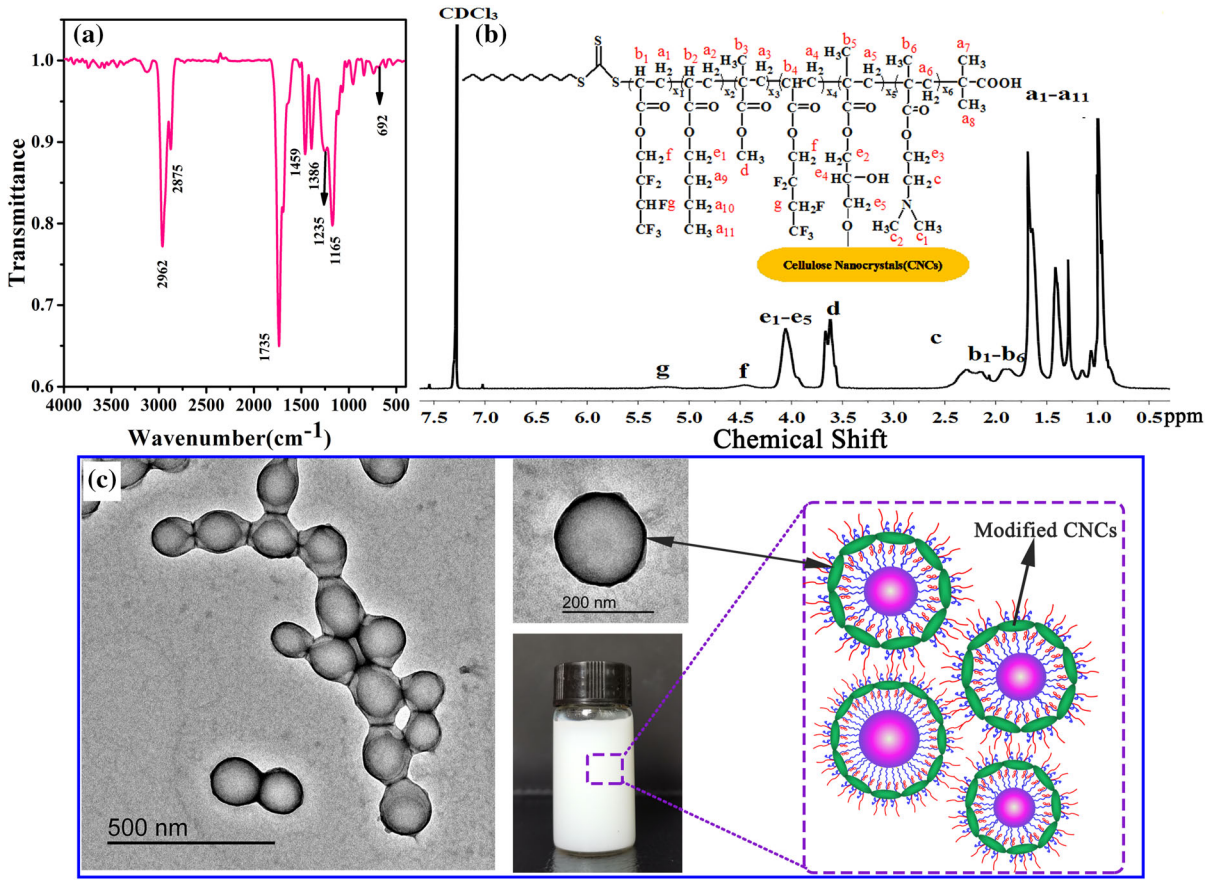

Fig. 1 **a** FT-IR and **b** ^{1}H-NMR spectra, and **c** TEM micrograph for the cellulose nanocrystal-dressed fluorinated polyacrylate latex particles

Pickering stabilizers were successfully incorporated into the fluorinated polyacrylate latex particles.

Effect of pH on pickering emulsion polymerization

Modified CNCs contain hydrophilic PDMAEMA segments and hydrophobic PHFBA segments, in which dimethylamino groups of the PDMAEMA segments can be protonated under acidic conditions to form quaternary ammonium groups with strong hydrophilicity (Darabi et al. 2016; Cunningham et al. 2016; Zhou et al. 2019). Consequently, the wettability of modified CNCs is sensitively dependent on pH value of the system, which will affect the synthesis and performance of emulsion (Yan and Masliyah 1996).

The results of Pickering emulsion polymerization measured in different pH values are shown in Fig. 2. When pH is 1.07, the monomer conversion is low and the gel rate is high, which may be ascribed to the combination of the following two aspects. Firstly, the PDMAEMA-g-CNC-g-PHFBA particles are more hydrophilic because more dimethylamino groups of PDMAEMA chains can be protonated at low pH value, which means that most nanoparticles reside in the water phase and are not adsorbed onto latex particles. Secondly, when HCl concentration is too high, the existence of excess HCl will suppress the thickness of the electric double layer, which results in insufficient electrostatic repulsion to prevent closer approach of the latex particles and finally leads to the coagulum (Zhou et al. 2014a). As a consequence, polymerization stability and monomer conversion are low. However, when the pH value increases to 2.06, the hydrophobicity and hydrophilicity of the PDMAEMA-g-CNC-g-PHFBA particles are relatively balanced and the wettability is moderate, meaning that more nanoparticles can be effectively adsorbed on the latex particle surface so as to improve

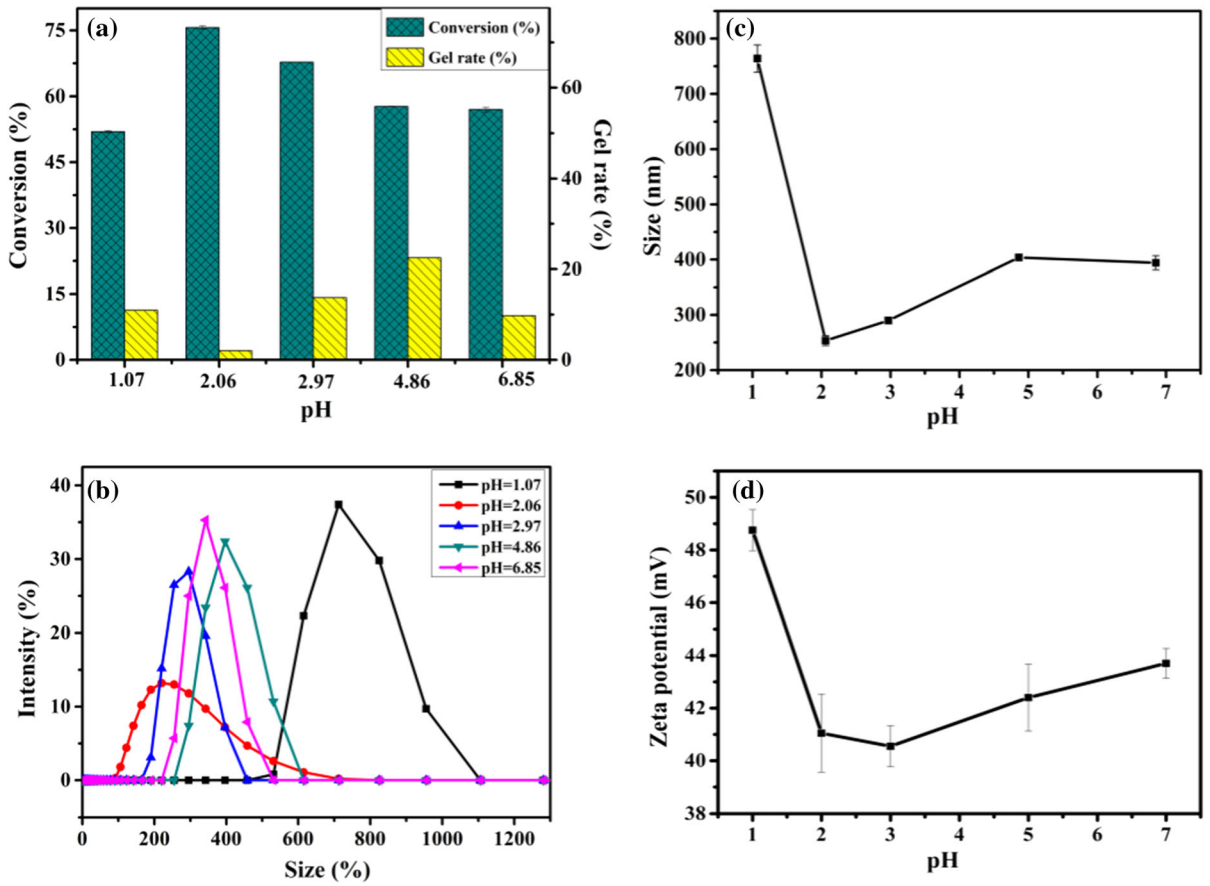

Fig. 2 Pickering emulsion polymerization at different pH values. **a** The monomer conversion and gel rate as a function of pH value, **b** particle size distribution as a function of pH value, **c** particle size and **d** zeta potential of latex particles as a function of pH value

the stability of emulsion polymerization. On this occasion, a high monomer conversion rate and a narrow latex particle size are reached. As pH value is more than 2.06, the dimethylamino groups have a relatively low degree of protonation, suggesting that the hydrophilic and hydrophobic equilibrium of the PDMAEMA-g-CNC-g-PHFBA particles is broken. In this case, the nanoparticle number adsorbed onto latex particle surface decreases, resulting in unstable polymerization (Valdez et al. 2017). On the other hand, the reduction of surface charge density of latex particles results in gradual weakening of mutual repulsion between latex particles, which promotes the coalescence of the small particles during the growth process (Tang et al. 2014). All these would be responsible for the formation of higher gel rate, larger particle size, and broader particle size distribution at high pH value.

In addition, the zeta potential measurement was utilized to characterize the stability of cellulose nanocrystal-dressed fluorinated polyacrylate emulsion. Typically, the colloidal system is regarded as stable when the absolute zeta potential of the system is greater than 30 mV (Dong et al. 2010; Zhou et al. 2017). Figure 2d shows the zeta potential of emulsion at different pH values. It is clearly seen that the zeta potentials of particles are all above + 30 mV, indicating a good stability of the cellulose nanocrystal-dressed fluorinated polyacrylate emulsion.

Effect of amount of fluorinated monomer on Pickering emulsion polymerization

In order to evaluate how fluorinated monomer affected monomer conversion, emulsion polymerization stability, and particle size and its distribution, a series of

experiments with different amounts of HFBA monomers were carried out as exhibited in Fig. 3. The monomer conversion increases with an increase of HFBA amount from 0 to 10wt%, and then decreases afterwards. Oppositely, the latex particle size decreases initially with an increase of HFBA amount, and then increases. In our system, the HFBA monomers can more easily enter into the interior of the latex particles because HFBA monomers have similar structure with the PHFBA segments in PDMAEMA-g-CNC-g-PHFBA particles. In the absence of HFBA monomers, mixed monomers have bad compatibility with PHFBA segments, it is difficult to maintain the polymerization stability, giving rise to high gel rate. With the increase of HFBA amount, the HFBA monomers enter into the interior of the latex particles, which promotes the micellar solubilization for monomers, and eventually, a more stable polymerization process is produced. Thus, the monomer conversion increases, and the gel rate and particle size decrease. On the contrary, when the HFBA amount is too high, the excess part of HFBA monomers will be unable to enter the latex particles and some of them can be homoploymerized. In addition, these homopolymers can form heterocoagulation with cellulose nanocrystal-dressed fluorinated polyacrylate latex particles through the intermolecular forces (Zhou et al. 2016), resulting in higher gel rate and larger particle size and distribution.

Water and oil resistance of the finished fabric

The water and oil resistance of the solid surface can be estimated by the contact angle measurement (Jiang et al. 2016; Qiao et al. 2017). Figure 4 shows the water contact angle (WCA) of the fabric finished by cellulose nanocrystal-dressed fluorinated polyacrylate emulsion. It could be clearly found that with the pH

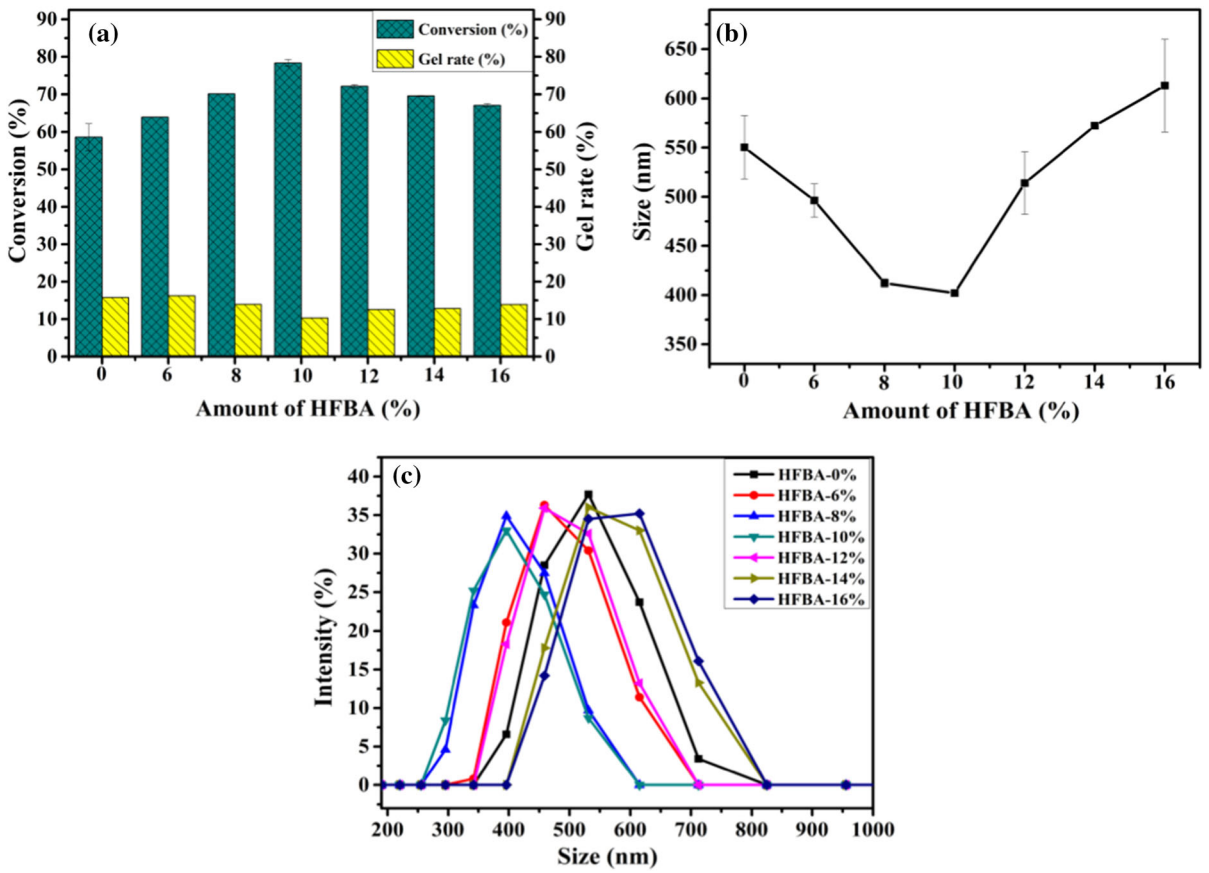

Fig. 3 Pickering emulsion polymerization with different amounts of HFBA. **a** the monomer conversion and gel rate as a function of HFBA amount, **b** latex particle size as a function of HFBA amount, **c** particle size distribution as a function of HFBA amount

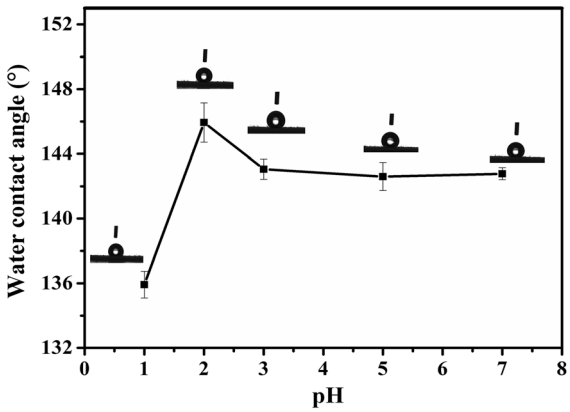

Fig. 4 Influence of pH value on contact angles of finished fabrics

value increasing, the WCA of the finished fabric obviously increases from 136.5° for pH = 1.07 to 146.5° for pH = 2.06. This change can be explained by the contribution of the increase of fluorinated segments in the polymer that result from the monomer conversion increase, as discussed in "Effect of pH on pickering emulsion polymerization" section. In the curing process, the composite emulsion can form the film on the fabric surface and the surface energy of the fabric would be reduced due to the low surface energy and strong hydrophobicity of the fluorinated groups, which can endow excellent water resistance for finished fabric (Chen et al. 2015b). However, with further increase in pH value from 2.06 to 6.85, the monomer conversion is relatively low, suggesting less fluorinated segments in the polymer, and thus the water resistance of finished fabric is weak.

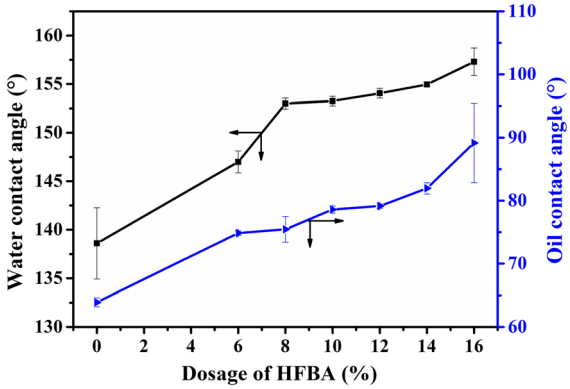

Fig. 5 Effect of amount of HFBA on contact angles of finished fabrics

The contact angles of fabrics finished with emulsions at different HFBA amounts are illustrated in Fig. 5. As shown in Fig. 5, the water and oil contact angles of the finished fabric increase with increasing HFBA content. The reason for this phenomenon is that the atomic content of F element on the surface of finished fabric increases accordingly with increasing fluorinated segments in the fluorinated polyacrylate. During the curing period, the surface energy of latex film on the finished fabric reduces because the fluorinated groups can spontaneously migrate and aggregate to the finished fabric surface, which causes the increase of the water and oil contact angles of the finished fabric.

Surface morphology of the finished fabric

The structure or morphology of polymer on substrates decides its application properties. Thus, it is significant to explore its morphology and chemical composition on the substrates. In this study, SEM measurement was employed to reveal the surface morphology of the unfinished fabric and the finished fabric. As presented in Fig. 6a, the surface of the unfinished fabric is uneven and has plenty of deep or slender concave grooves. However, the grooves of the fabric finished with cellulose nanocrystal-dressed fluorinated polyacrylate emulsion are almost obscured by the polymer film. Moreover, some granular convex structures can be visualized on the finished fabric surface (Fig. 6b), and a possible reason for this is the presence of CNC nanoparticles (Yao et al. 2019). EDX measurement was used to characterize the content and distribution of elements on the surface of the fabric finished by cellulose nanocrystal-dressed fluorinated polyacrylate emulsion (Fig. 7). It is shown that the elements of C, N, O, and F are evenly deposited on the entire fabric surface, which means that cellulose nanocrystal-dressed fluorinated polyacrylate latex particles were uniformly spread onto the finished fabric. In this experiment, we also found the unfinished fabric was very hydrophilic and the water droplets could completely penetrate into the fabric after 2 s, while the water contact angle of the finished fabric was up to 153.3°. This result demonstrates that the finished fabric has excellent water resistance, which can be attributed to the synergistic effect of the rough surface from CNC nanoparticles and the low surface energy of the fluorinated polyacrylate (Baidya

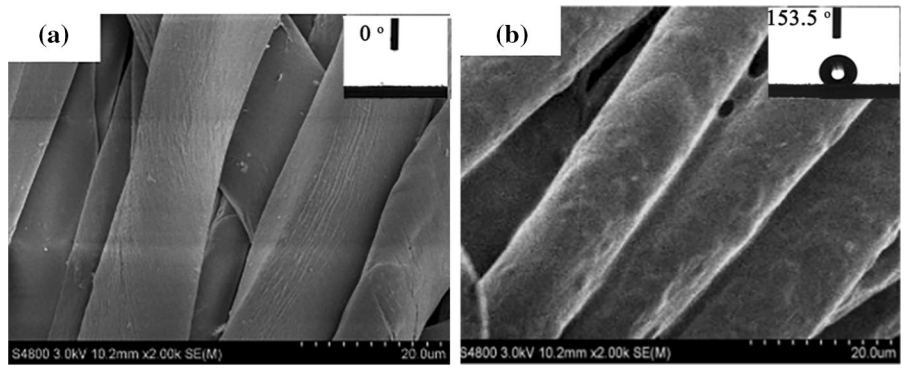

Fig. 6 **a** SEM images of the unfinished fabric and **b** the fabric finished with cellulose nanocrystal-dressed fluorinated polyacrylate emulsion

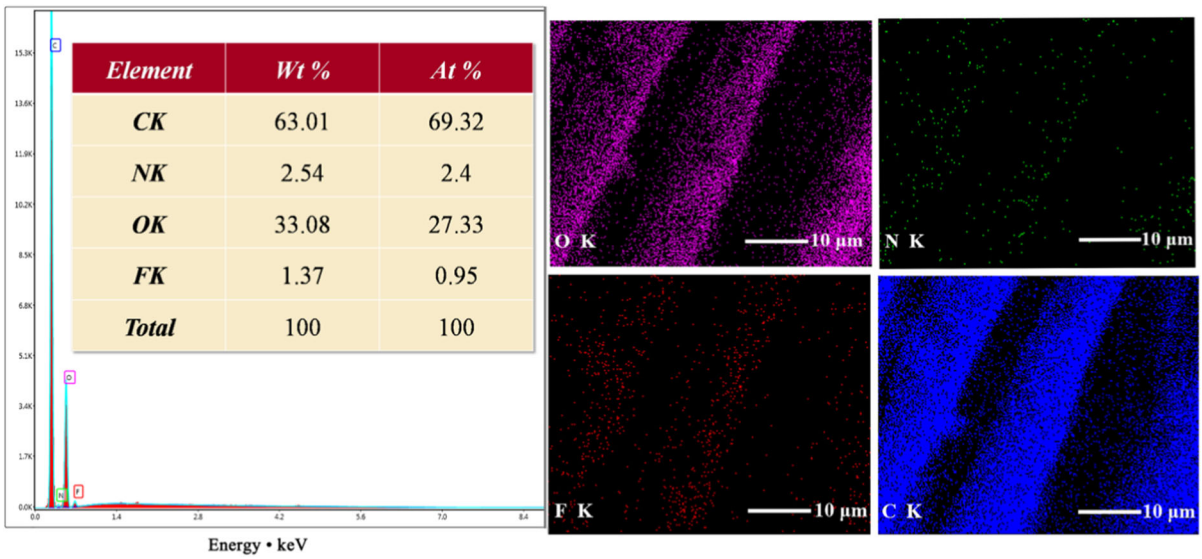

Fig. 7 EDX and the element mapping of the fabric finished with cellulose nanocrystal-dressed fluorinated polyacrylate emulsion

et al. 2018; Khanjani et al. 2018; Zhi et al. 2017; Martin and Bhushan 2017; Xu et al. 2019).

Conclusion

We prepared cellulose nanocrystal-dressed fluorinated polyacrylate latex particles by a RAFT-mediated Pickering emulsion polymerization process. The pH values and the amount of HFBA were crucial factors that affected polymerization stability. The good polymerization stability and narrow particle size distribution were obtained when the amount of HFBA was 10% and the pH value was 2.06. Contact angle experiments revealed that the finished fabrics had excellent resistance to water and oil. In addition, the latex particles presented a well-defined core–shell structure with modified CNCs as the shell and fluorinated polyacrylate as the core. The SEM and EDX analysis indicated that cellulose nanocrystal-dressed fluorinated polyacrylate latex particles were uniformly coated on the finished fabrics. Overall, this is an attractive and versatile synthetic method to obtain CNC-based polymers for coating applications.

Acknowledgments We thank National Natural Science Foundation of China (Nos. 21978162 and 21206088), Shaanxi Provincial Natural Science Foundation of China (No. 2017JZ003), National Demonstration Center for Experimental Light Chemistry Engineering Education Open Project (No. 2018QGSJ02-15), and Science and Technology Plan of Xi'an

City (No. 2019216514GXRC001CG002-GXYD1.3) for supporting this research.

References

Baidya A, Das SK, Ras RHA, Pradeep T (2018) Fabrication of a waterborne durable superhydrophobic material functioning in air and under oil. Adv Mater Interfaces. https://doi.org/10.1002/admi.201701523

Chen A, Blakey I, Jack KS, Whittaker AK, Peng H (2015a) Control through monomer placement of surface properties and morphology of fluoromethacrylate copolymers. J Polym Sci, Part A: Polym Chem 53:2633–2641

Chen X, Zhou JH, Ma JZ (2015b) Synthesis of a cationic fluorinated polyacrylate emulsifier-free emulsion via ab initio RAFT emulsion polymerization and its hydrophobic properties of coating films. RSC Adv 5:97231–97238

Chen QH, Zheng J, Xu YT, Yin SW, Liu F, Tang CH (2018) Surface modification improves fabrication of Pickering high internal phase emulsions stabilized by cellulose nanocrystals. Food Hydrocolloids 75:125–130

Cherhal F, Cousin F, Capron I (2016) Structural description of the interface of Pickering emulsions stabilized by cellulose nanocrystals. Biomacromol 17:496–502

Clélia M, Bruno J (2014) Nanocellulose/polymer multilayered thin films: tunable architectures towards tailored physical properties. Nord Pulp Pap Res J 29:19–30

Cunningham MF, Jessop PG (2016) An introduction to the principles and fundamentals of CO_2-switchable polymers and polymer colloids. Eur Polym J 76:208–215

Darabi A, Jessop PG, Cunningham MF (2016) CO_2-responsive polymeric materials: synthesis, self-assembly, and functional applications. Chem Soc Rev 45:4391–4436

Dong XQ, Xu J, Cao CB, Sun DJ, Jiang XR (2010) Aqueous foam stabilized by hydrophobically modified silica particles and liquid paraffin droplets. Colloid Surf A, Physicochem Eng Asp 353:181–188

Du WB, Guo J, Li HM, Gao Y (2017a) Heterogeneously modified cellulose nanocrystals-stabilized Pickering emulsion: preparation and their template application for the creation of PS microspheres with amino-rich surfaces. ACS Sustain Chem Eng 5:7514–7523

Du X, Zhang Z, Liu W, Deng YL (2017b) Nanocellulose-based conductive materials and their emerging applications in energy devices: a review. Nano Energy 35:299–320

Errezma M, Mabrouk AB, Magnin A, Dufresne A, Boufi S (2018) Surfactant-free emulsion Pickering polymerization stabilized by aldehyde-functionalized cellulose nanocrystals. Carbohydr Polym 202:621–630

El-Fattah MA, Hasan AMA, Keshawy M, El Saeed AM (2018) Nanocrystalline cellulose as an eco-friendly reinforcing additive to polyurethane coating for augmented anticorrosive behavior. Carbohydr Polym 183:311–318

Habibi Y, Lucia LA, Rojas OJ (2010) Cellulose nanocrystals: chemistry, self-assembly, and applications. Chem Rev 110:3479–3500

Jiang YJ, Li L, Liu JP, Wang R, Wang HS, Tian Q, Li XY (2016) Hydrophobic films of acrylic emulsion by incorporation of fluorine-based copolymer prepared through the RAFT emulsion copolymerization. J Fluorine Chem 183:82–91

Kannan KC, Corsolini S, Falandysz J, Oehme G, Focardi S, Giesy JP (2002) Perfluorooctanesulfonate and related fluorinated hydrocarbons in marine mammals, fishes, and birds from coasts of the Baltic and the Mediterranean Seas. Environ Sci Technol 36:3210–3216

Khanjani P, Thomas King AW, Partl GJ, Johansson LS, Kostiainen MA, Ras RHA (2018) Superhydrophobic paper from nanostructured fluorinated cellulose esters. ACS Appl Mater Interfaces 10:11280–11288

Li F, Mascheroni E, Piergiovanni L (2015) The potential of nanocellulose in the packaging field: a review. Packag Technol Sci 28:475–508

Li X, Li J, Gong J, Kuang YS, Mo LH (2018) Cellulose nanocrystals (CNCs) with different crystalline allomorph for oil in water Pickering emulsions. Carbohydr Polym 183:303–310

Liang JY, He L, Zuo YY, Chen ZY, Peng T (2018) An insight into the amphiphobicity and thermal degradation behavior of PDMS-based block copolymers bearing POSS and fluorinated units. Soft Matter 14:5235–5245

Lizundia E, Fortunati E, Dominici F, Vilas JL, León LM, Armentano I, Torre L, Kenny JM (2016) PLLA-grafted cellulose nanocrystals: role of the CNC content and grafting on the PLA bionanocomposite film properties. Carbohydr Polym 142:105–113

Lv C, Cui K, Li SC, Wu HT, Ma Z (2016) Polystyrene-*b*-poly(2,2,2-trifluoroethyl acrylate)-*b*-polystyrene copolymers: synthesis and fabrication of their hydrophobic porous films, spheres, and fibers. J Polym Sci, Part A: Polym Chem 54:678–685

Martin JW, Smithwick MM, Braune BM, Hoekstra PF, Muir DCG, Mabury SA (2004) Identification of long-chain perfluorinated acids in biota from the Canadian Arctic. Environ Sci Technol 38:373–380

Martin S, Bhushan B (2017) Transparent, wear-resistant, superhydrophobic and superoleophobic poly(dimethylsiloxane) (PDMS) surfaces. J Colloid Interface Sci 488:118–126

Mougel JB, Bertoncini P, Cathala B, Chauvet O, Capron I (2019) Macroporous hybrid Pickering foams based on carbon nanotubes and cellulose nanocrystals. J Colloid Interface Sci 544:78–87

Moustafa H, Youssef AM, Darwish NA, Abou-Kandil AI (2019) Eco-friendly polymer composites for green packaging: future vision and challenges. Compos Part B: Eng 172:16–25

Ng HM, Sin LT, Tee TT, Bee ST, Hui D, Low CY, Rahmat AR (2015) Extraction of cellulose nanocrystals from plant sources for application as reinforcing agent in polymers. Compos Part B: Eng 75:176–200

Qiao Z, Qiu T, Liu WW, Zhang LD, Tu JQ, Guo LH, Li XY (2017) A "green" method for preparing ABCBA pentablock elastomers by using RAFT emulsion polymerization. Polym Chem 8:3013–3021

Scaffaro R, Botta L, Lopresti F, Maio A, Sutera F (2016) Polysaccharide nanocrystals as fillers for PLA based nanocomposites. Cellulose 24:447–478

Tang JT, Lee MFX, Zhang W, Zhao BX, Berry RM, Tam KC (2014) Dual responsive Pickering emulsion stabilized by

poly[2-(dimethylamino)ethyl methacrylate] grafted cellulose nanocrystals. Biomacromol 15:3052–3060

Tang CX, Chen YM, Luo JH, Low MY, Shi ZQ, Tang JT, Zhang Z, Peng BL, Tam KC (2019) Pickering emulsions stabilized by hydrophobically modified nanocellulose containing various structural characteristics. Cellulose 26:7753–7767

Valdez OG, Brescacin T, Arredondo J, Bouchard J, Jessop PG, Champagne P, Cunningham MF (2017) Grafting CO_2-responsive polymers from cellulose nanocrystals via nitroxide-mediated polymerisation. Polym Chem 8:4124–4131

Wang ZH, Carlsson DO, Tammela P, Hua K, Zhang P, Nyholm L, Strømme M (2015) Surface modified nanocellulose fibers yield conducting polymer-based flexible supercapacitors with enhanced capacitances. ACS Nano 9:7563–7571

Werner A, Schmitt V, Sèbe G, Héroguez V (2017) Synthesis of surfactant-free micro- and nanolatexes from Pickering emulsions stabilized by acetylated cellulose nanocrystals. Polym Chem 8:6064–6072

Xu T, Xiao QQ, Chen JY, Li L, Yang XJ, Liu LF, Yuan WH, Zhang BJ, Wu HJ (2019) Hydrophobicity of polyacrylate emulsion film enhanced by introduction of nano-SiO_2 and fluorine. Polymers. https://doi.org/10.3390/polym11020255

Xu W, An QF, Hao LF, Zhang D, Zhang M (2014) Synthesis of self-crosslinking fluorinated polyacrylate soap-free latex and its waterproofing application on cotton fabrics. Fiber Polym 15:457–464

Yan N, Masliyah JH (1996) Effect of pH on adsorption and desorption of clay particles at oil-water interface. J Colloid Interface Sci 181:20–27

Yao HT, Zhou JH, Li H, Zhao JJ (2019) Nanocrystalline cellulose/fluorinated polyacrylate latex via RAFT-mediated surfactant-free emulsion polymerization and its application as waterborne textile finishing agent. J Polym Sci, Part A: Polym Chem 57:1305–1314

Zhang QH, Wang QY, Zhan XL, Chen FQ (2014) Synthesis and performance of novel fluorinated acrylate polymers: preparation and reactivity of short perfluoroalkyl group containing monomers. Ind Eng Chem Res 53:8026–8034

Zhang CF, Xu TT, Bao ZB, Fu ZG, Chen LJ (2016) Synthesis and characterization of polyacrylate latex containing fluorine and silicon via semi-continuous seeded emulsion polymerization. J Adhes Sci Technol 31:1658–1670

Zhi DF, Lu Y, Sathasivam S, Parkin IP, Zhang X (2017) Large-scale fabrication of translucent and repairable superhydrophobic spray coatings with remarkable mechanical, chemical durability and UV resistance. J Mater Chem A 5:10622–10631

Zhou JH, Zhang L, Ma JZ (2013) Fluorinated polyacrylate emulsifier-free emulsion mediated by poly(acrylic acid)-*b*-poly(hexafluorobutyl acrylate) trithiocarbonate via ab initio RAFT emulsion polymerization. Chem Eng J 223:8–17

Zhou JH, Wang HL, Zhang L, Ma JZ (2014a) Ab initioreversible addition-fragmentation chain transfer emulsion polymerization of styrene/butyl acrylate mediated by poly(acrylic acid)-block-polystyrene trithiocarbonate. Polym Int 63:2098–2104

Zhou JH, Wang LB, Cui YJ, Ma JZ (2014b) Synthesis and properties of nano-TiO_2 modified fluorine-containing polyacrylate soap-free emulsion. Mater Sci Forum 809–810:161–168

Zhou JH, Chen X, Duan H, Ma JZ, Ma YR (2015) Synthesis and characterization of nano-SiO_2 modified fluorine-containing polyacrylate emulsifier-free emulsion. Appl Surf Sci 331:504–511

Zhou JH, Chen X, Ma JZ (2016) Cationic fluorinated polyacrylate emulsifier-free emulsion mediated by poly(2-(dimethylamino) ethyl methacrylate)-*b*-poly(hexafluorobutyl acrylate) trithiocarbonate via ab initio RAFT emulsion polymerization. Prog Org Coat 100:86–93

Zhou JH, Chen X, Ma JZ (2017) Synthesis of cationic fluorinated polyacrylate copolymer by RAFT emulsifier-free emulsion polymerization and its application as waterborne textile finishing agent. Dyes Pigments 139:102–109

Zhou JH, Yao HT, Ma JZ (2018) Recent advances in RAFT-mediated surfactant-free emulsion polymerization. Polym Chem 9:2532–2561

Zhou JH, Li YN, Li H, Yao HT (2019) Cellulose nanocrystals/fluorinated polyacrylate soap-free emulsion prepared via RAFT-assisted Pickering emulsion polymerization. Colloid Surf B, Biointerfaces 177:321–328